Enhancing the Electrical Conductivity of Carbon-Nanotube-Based Transparent Conductive Films Using Functionalized Few-Walled Carbon Nanotubes Decorated with Palladium Nanoparticles as Fillers

Yu-An Li,[†] Nyan-Hwa Tai,[†,‡,*] Swe-Kai Chen,[‡] and Tsung-Yen Tsai[†]

[†]Department of Materials Science and Engineering and [‡]Center for Nanotechnology, Materials Science and Microsystems, National Tsing Hua University, Hsinchu 30013, Taiwan

ABSTRACT This work demonstrates the processing and characterization of the transparent and highly electrically conductive film using few-walled carbon nanotubes (FWCNTs) decorated with Pd nanoparticles as fillers. The approach included functionalizing the FWCNTs, immersing them in an aqueous solution of palladate salts, and subsequently subjecting them to a reduction reaction in H_2. Field-emission scanning electron microscopy and transmission electron microscopy images showed that the functionalized FWCNTs (f-FWCNTs) were decorated with uniform and homogeneous Pd nanoparticles with an average diameter of 5 nm. A shift of the G-band to a higher frequency in the Raman spectra of the Pd-decorated f-FWCNTs (Pd@f-FWCNTs) illustrates that the p-type doping effect was enhanced. X-ray photoelectron spectroscopy and energy-dispersive X-ray spectroscopy showed that $PdCl_2$ was the primary decoration compound on the f-FWCNTs prior to the reduction reaction and that Pd nanoparticles were the only decorated nanoparticles after H_2 reduction. The contact resistance between the metallic materials and the semiconducting CNTs in FWCNTs, controlled by the Schottky barrier, was significantly decreased compared to the pristine FWCNTs. The decrease in contact resistance is attributed to the 0.26 eV increase of the work function of the Pd@f-FWCNTs. Extremely low sheet resistance of 274 ohm/sq of the poly(ethylene terephthalate) substrates coated with Pd@f-FWCNTs was attained, which was 1/25 the resistance exhibited by those coated with FWCNTs, whereas the same optical transmittance of 81.65% at a wavelength of 550 nm was maintained.

KEYWORDS: carbon nanotubes · transparent conductive film · p-type doping effect · palladium decoration · work function

Indium tin oxide (ITO) is a well-known transparent conductive material that is typically applied to electronic devices,[1,2] displays,[3] and photovoltaic devices[4] because of its low electrical resistivity and high optical transmittance. Because of the rapid consumption of indium oxide raw materials, efforts have been made to develop new materials to substitute for ITO, such as fluorine-doped tin oxide,[5,6] aluminum-doped zinc oxide,[7] and other transparent conductive oxide materials.[8] However, these materials do not perform better than ITO and are difficult to process; in addition, they are hard, brittle, and easily detrimental, resulting in an increase in electric resistance or circuit damage when used in flexible devices.[9] To fabricate a conductive layer for flexible devices, such as organic light-emitting diodes, organic photovoltaics, e-paper, and touch screens, several conductive polymers have been developed.[10−12] Poly(3,4-ethylenedioxythiophene)-poly(4-stryrenesulfonate) (PEDOT:PSS) is a popular conductive polymer, but PEDOT:PSS exhibits a light blue color and has the disadvantages of weak thermal stability and poor UV resistance.[13]

Carbon nanotubes (CNTs) are considered one of the candidates for flexible transparent conductive films because of their unique properties, such as superior chemical stability, a high aspect ratio, excellent electron transfer, and mechanical flexibility.[14] Many attempts have been made to enhance the optoelectronic properties of CNT-based transparent conductive films (CNT-TCFs), including the immersion of CNT-TCFs in an acid solution,[15−17] the mixing of CNTs with a conductive polymer,[18] and the generation of CNT network bridges.[19] However, very limited improvement in optoelectronic properties has been reported.

This work proposes a simple method for the preparation of CNT-TCFs using functionalized few-walled carbon nanotubes (f-FWCNTs)

* Address correspondence to nhtai@mx.nthu.edu.tw.

Received for review May 18, 2011 and accepted July 24, 2011.

Published online July 25, 2011
10.1021/nn201824h

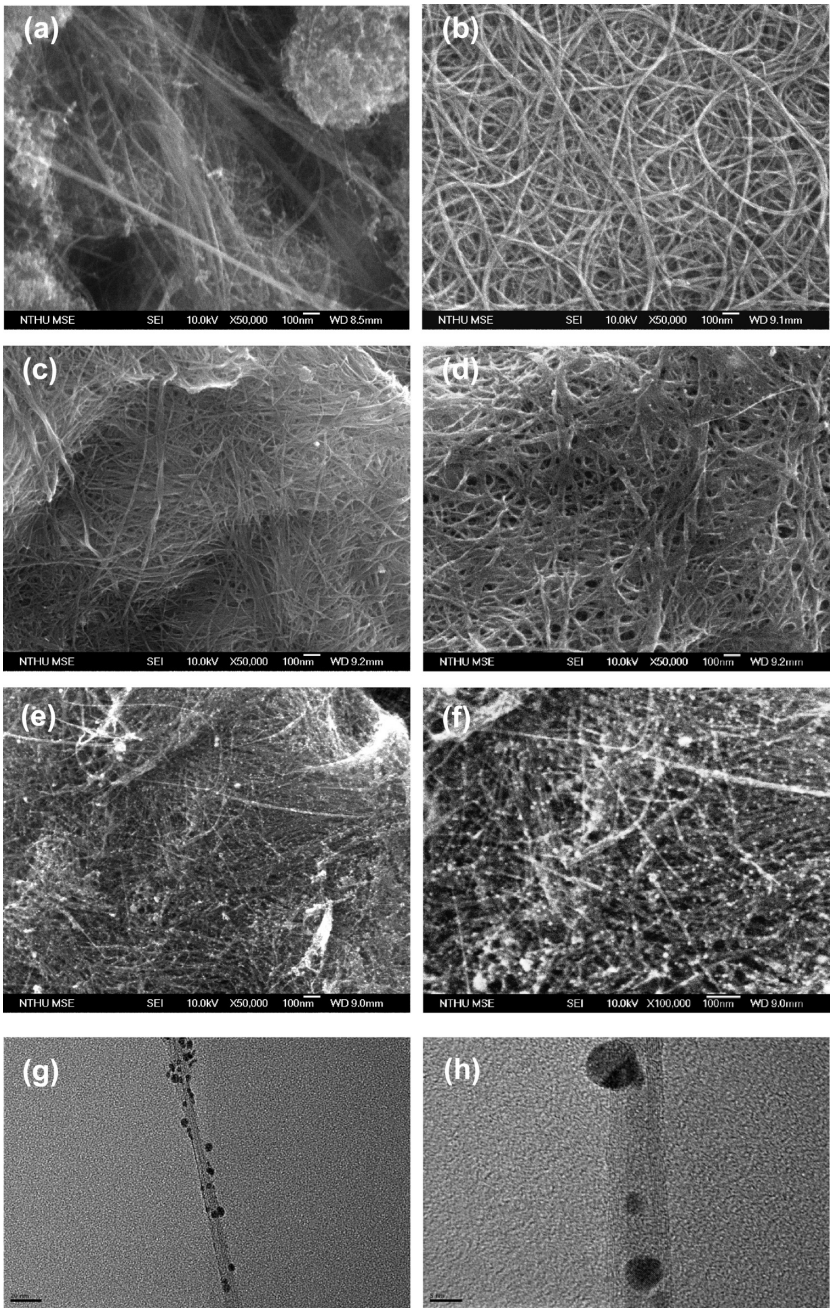

Figure 1. FESEM images of (a) the as-purchased pristine FWCNTs; (b) p-FWCNTs; (c) f-FWCNTs; (d) $PdCl_2$@f-FWCNTs; (e) Pd@f-FWCNTs; and (f) high magnification of panel e. TEM images of Pd@f-FWCNTs at low (g) and high (h) magnification.

decorated with Pd nanoparticles (Pd@f-FWCNTs) as the primary additive without any post-treatment. The Pd@f-FWCNTs were derived from the hydrogen reduction of palladate salts on f-FWCNTs, where Pd has been verified to exhibit good wetting properties.[20] In this work, we found FWCNTs, due to unique structure, possess more advantages than single-walled (SWCNTs) and multiwalled CNTs (MWCNTs). SWCNTs have very narrow diameters which benefits the optical transmittance; however, SWCNTs show one-third as metallic and two-thirds as semiconducting depending on their chirality. Therefore, the presence of the semiconducting SWCNTs may increase the contact electrical resistance. MWCNTs possess good electrical conductivity due to their more conductive π channels; however, the thick diameter decreases the optical performance.[21] FWCNTs perform the conducting and transmittance properties with a more balance result, which is suitable for preparing transparent conductive thin film. Compared to previously published results for decorating metal nanoparticles on the surface of CNTs, our proposed method is simple because it does not require a bridging material, such as 4-aminobenzene monolayer, for adhering Pd particles to the CNTs'

TABLE 1. Semiquantitative Analysis Based on EDX for CNTs Subjected to Different Treatments

	weight (%)				atomic (%)			
material	C K	O K	Cl K	Pd L	C K	O K	Cl K	Pd L
Pristine FWCNTs[a]	85.68	10.72			90.93	8.53		
p-FWCNTs	100				100			
f-FWCNTs	71.55	28.45			77.01	22.99		
$PdCl_2$@f-FWCNTs	25.02	14.24	16.71	44.03	54.02	23.05	12.21	10.72
Pd@f-FWCNTs	40.14	8.11		51.75	77.11	11.68		11.21

[a] The pristine FWCNTs have other signals at 0.20 of Cr K, 0.42 of Co K, and 2.98 of Mo L in weight ratio; 0.05 of Cr K, 0.09 of Co K, and 0.40 of Mo L in atomic ratio. These signals result from catalysts in the pristine FWCNTs.

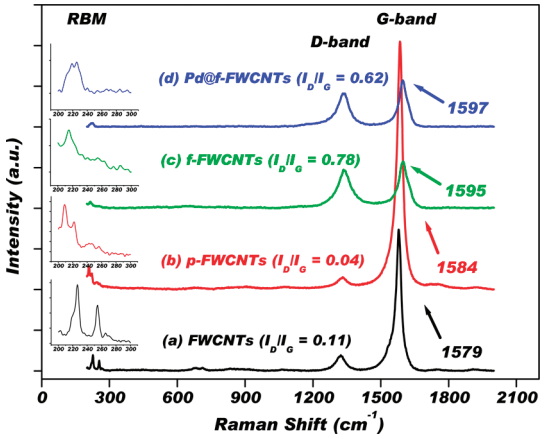

Figure 2. Raman spectra of (a) pristine FWCNTs, (b) p-FWCNTs, (c) f-FWCNTs, and (d) Pd@f-FWCNTs. The arrows indicate the G-band of the Raman shift. The shift of the G-band from 1579 cm^{-1} for FWCNTs to 1597 cm^{-1} for Pd@f-FWCNTs is attributed to the p-type doping effect induced by Pd decoration. Insets show the radial breathing modes (RBM) of each sample.

surface.[22] The bridging material needs to be removed after the Pd decoration reaction, because it has a negative effect on electrical conductivity. The use of high-energy radiation, such as γ-irradiation, to reduce metal ions to metal has also been reported.[23] However, the high-energy radiation may damage the CNTs and result in an increase in their electrical resistance. Several studies regarding the metal coating on CNTs for the production of flexible transparent conducting films have been reported. Park *et al.* reported the optoelectronic performance of Au nanoparticles-decorated MWCNTs using the ionic liquid-assisted sonochemical method, they produced the film with sheet resistance and transmittance of 19.4×10^3 ohm/sq and 79.6%, respectively.[24] Yang *et al.* reported the coating of Au nanoparticles on double-walled CNT (DWCNT) film. The performance of the DWCNT film with sheet resistance of ~600 ohm/sq and transmittance of 83% was achieved when the DWCNT film was immersed into Au salt solution for 10 min.[25] Liu *et al.* revealed the synthesis of flexible and transparent conductive film of CNT/graphene network coordinated by divalent metal ions. They reported a low sheet resistance of 680 ohm/sq with a high transmittance of 86% of the film. The sheet resistance was further decreased to 370 ohm/sq while only 1% loss in transmittance when $SOCl_2$ was used as the chemical doping reagent.[26] The proposed method in this study not only generates more contact area among Pd@f-FWCNTs for electron transfer within the film, but also enhances the conductivity due to an increase in the work function resulting from Pd doping by using simple process. Our results show that the electrical sheet resistance of the CNT-TCFs at the same optical transmittance can be reduced significantly to 1/25 the resistance of those without Pd doping. The high conductive CNT-based thin transparent film can be used in electrode of touch panel, flexible display, solar cell, EMI shielding, and antistatic application.

RESULTS AND DISCUSSION

The field emission scanning electron microscopy (FESEM) images of the FWCNTs after various treatments are shown in Figure 1. Many carbonaceous impurities and catalyst aggregations in the pristine FWCNTs were observed in the images, as shown in Figure 1a. After purification under air at 600 °C, most of the impurities were removed, and purified FWCNTs (p-FWCNTs) with entangled structures were obtained (Figure 1b). To increase the active sites and to produce functional groups with negative charges, such as carboxyl groups, on the surface of p-FWCNTs, the p-FWCNTs were oxidized using strong acids. The products were designated as f-FWCNTs, as shown in Figure 1c. After immersing the f-FWCNTs in an aqueous solution of palladate salts, followed by filtrating and drying, the diameter of the f-FWCNT bundles increased. Palladium and palladium dichloride ($PdCl_2$) were coated on the surface of f-FWCNTs (Figure 1d; the details of characterization will be discussed in the next section). After hydrogen reduction, many spherical nanoparticles of uniform size were adhered to the f-FWCNT surface, as shown in Figure 1e,f. The transmission electron microscopy (TEM) images depict the uniform and homogeneous dispersion of the spherical Pd nanoparticles, which exhibit an average particle diameter of 5 nm (Figure 1g,h).

The semiquantitative analysis results based on the energy-dispersive X-ray spectroscopy (EDX) spectrum is depicted in Table 1. The results for pristine FWCNTs show that the sums of the weight and atomic ratios are not 100%, which is attributed to the presence of other catalyst particles such as Cr, Co, and Mo; a detailed explanation is given in the footnote of Table 1. After purification, only a C signal was detected. After the reaction of the f-FWCNTs with Na_2PdCl_4, Pd and $PdCl_2$ were decorated on the surface of the f-FWCNTs, which are designated as $PdCl_2$@f-FWCNTs. As shown in

Table 1, 12.21 atom % of Cl corresponds to 6.11 atom % of Pd because of the presence of $PdCl_2$ molecules, and 4.61 atom % of Pd was estimated as a residual Pd particle because the total atomic ratio of Pd is 10.72 atom % (10.72 − 6.11 = 4.61). After hydrogen reduction, some of the Pd nanoparticles formed because of an *in situ* reduction of $PdCl_2$, whereas other Pd nanoparticles retained their original state. Furthermore, the total atomic ratios of Pd before and after the hydrogen reduction are approximately the same, which indicates that no Pd was removed.

Figure 2 illustrates the Raman spectra of the CNTs after different steps of the experimental treatments. The spectrum of pristine FWCNTs shows three major signals, including radial breathing modes (RBM), disorder (D-band), and graphitic signals (G-band). The presence of RBM indicates that the FWCNTs are mingled with SWCNTs, and the SWCNTs in the FWCNTs may present metallic or semiconducting behavior, depending on the chirality of SWCNTs. Peaks at 1330 and 1580 cm^{-1} present the D-band and G-band, respectively. The D-band forms because of the disordered structure, defects, amorphous carbon species, and impurities in the FWCNTs. The ratio of the intensities of the D- and G-bands (I_D/I_G) is a useful index to express the degree of graphitization of CNTs. The smaller the I_D/I_G ratio, the higher the graphitic structure of the CNTs. The I_D/I_G values of FWCNTs, p-FWCNTs, f-FWCNTs, and Pd@f-FWCNTs are 0.11, 0.04, 0.78, and 0.62, respectively. After oxidation in air at 600 °C, the D-band decreased because most of the disordered carbon species were removed from the FWCNTs; however, the temperature was not sufficiently high to remove all the disordered carbon species. The increase in I_D/I_G for the f-FWCNTs is a consequence of the presence of the damaged CNTs that resulted from the acid treatment of the functional groups on the FWCNT walls, which implies that the acid treatment can partially destroy the graphitic structure. However, the I_D/I_G ratio of the Pd@f-FWCNTs (0.62) is lower than that of the f-FWCNTs (0.78), which illustrates that Pd nanoparticles occupied the destroyed sites on the surfaces of the FWCNTs. In addition, the G-band peak shifted from 1579 cm^{-1} for FWCNTs to 1597 cm^{-1} for Pd@f-FWCNTs indicating that Pd decoration induces the phonon-stiffening effect due to a p-type doping effect.[27−29] The p-type doping effect creates more "holes" because the dopant material accepts electrons from the neighboring atoms, thereby producing holes in the neighboring atoms. Therefore, the formation of holes increases the electron density, as well as the electrical conductivity.

The chemical characteristics of the carbon surface affect Pd and $PdCl_2$ decoration.[30,31] If the carbon surface contains functional groups with negative charges, such as COO^-, the surface can be decorated with Pd^{2+} ions and form COO^-—Pd^{2+} bonds. However, the graphitic surface will be decorated with $PdCl_2$ because the positive charge of $C_\pi H_3O^+$ on the basal plane of the graphite can form $C_\pi H_3O^+$—$PdCl_4^{2-}$ bonds, depending on the nature of the electrostatic forces on the carbon surface. Therefore, Pd and $PdCl_2$ decoration may occur simultaneously because of the coexistence of the COO^- functional groups and the π-bonding

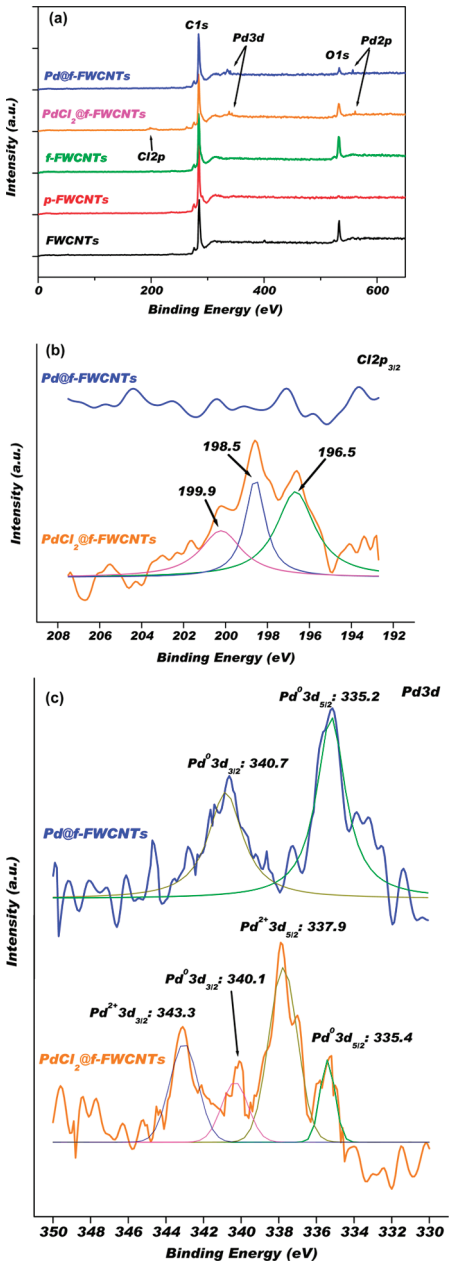

Figure 3. XPS spectra of (a) the spectral region from 0 to 650 eV, (b) the chlorine 2p region, and (c) the palladium 3d region. For $PdCl_2$@f-FWCNTs in panel b, the Cl2p is fitted with three peaks: 196.5 eV for ionic (Cl^-), 198.5 eV for Pd−Cl bonds (Cl*), and 199.9 eV for covalent species (−Cl).[32] In panel c, the Pd3d curves are fitted with two major peaks: $Pd3d_{5/2}$ and $Pd3d_{3/2}$. The $PdCl_2$@f-FWCNTs exhibits four peaks at 335.4, 337.9, 340.1, and 343.3 eV. The Pd metal and $PdCl_2$ coexist in the $PdCl_2$@f-FWCNTs.[31,32] The binding energy was calibrated using the C1s photoelectron peak at 284.6 eV as reference.

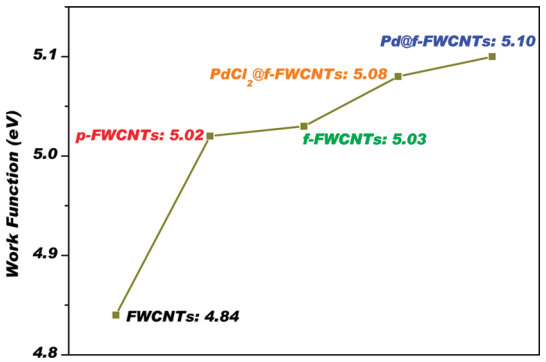

Figure 4. Variations of the work functions of CNTs after different treatments.

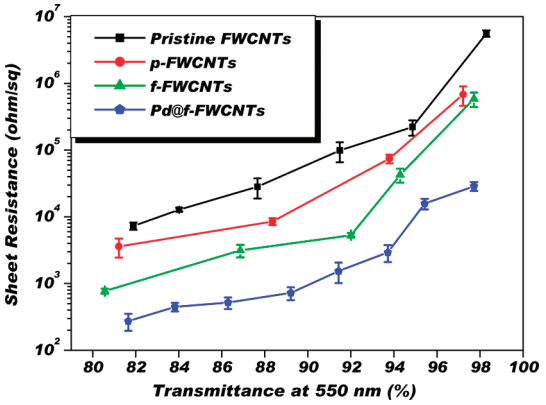

Figure 5. Comparison of the electrical sheet resistance and optical transmittance at a wavelength of 550 nm. The sheet resistance decreased from 6998 ohm/sq for the pristine FWCNTs (estimated by extrapolation) to 274 ohm/sq for the Pd@f-FWCNTs, with a corresponding transmittance of 81.65%.

orbitals of $C_\pi H_3O^+$ on the f-FWCNT surface.[30] On the basis of the Raman spectra shown in Figure 2, the intensity of the G-band is always higher than that of the D-band, which indicates the existence of substantial $C_\pi H_3O^+$ charges on the f-FWCNT surface. Therefore, it is expected that the amount of $PdCl_2$ decoration is higher than the amount of Pd decoration prior to hydrogen reduction. This presumption is consistent with the EDX data presented in Table 1.

On the basis of the X-ray photoelectron spectroscopy (XPS) results depicted in Figure 3, the electronic state of the FWCNTs, with and without decoration, can be identified. As shown in Figure 3a, O1s can be detected by attributing the presence of hydroxyl groups to moisture and the presence of carboxyl groups to the acid treatment of FWCNTs and f-FWCNTs. For p-FWCNTs, only C1s can be detected because the purification process performed at 600 °C removed most of the amorphous carbon and induced graphitic crystallization of the FWCNTs (I_D/I_G is 0.04). Hence, only few sites act as moisture-absorbing sites on the FWCNT surface, which results in no O1s signal in the p-FWCNT's curve depicted in Figure 3a. This result is also consistent with the EDX results shown in Table 1.

Pd2p and Pd3d were detected in both $PdCl_2$@f-FWCNTs and Pd@f-FWCNTs, but only Cl2p was observed in $PdCl_2$@f-FWCNTs, which indicates that the Cl was completely removed after reduction by hydrogen gas. Three fitted peaks, located at 196.5, 198.5, and 199.9 eV, appear in the XPS of $PdCl_2$@f-FWCNTs, as shown in Figure 3b; the Cl2p peaks at 196.5 and 199.9 eV correspond to the ionic (Cl^-) and covalent (−Cl) chlorine species, respectively. The peak at 198.5 eV suggests the formation of a Pd−Cl bond.[32] As previously discussed, the peak of Cl2p disappeared after H_2 reduction during the synthesis of Pd@f-FWCNTs.

Figure 3c shows the enlarged XPS spectra of Pd3d. Four major peaks, located at 335.4, 337.9, 340.1, and 343.3 eV, for $PdCl_2$@f-FWCNTs were detected. The four peaks can be divided into two chemical states.[31,32] The peaks at 335.4 and 340.1 eV represent metallic states of $Pd^0 3d_{5/2}$ and $Pd^0 3d_{3/2}$, respectively; the peaks at 337.9 and 343.3 eV represent ionic states of $Pd^{2+} 3d_{5/2}$ and $Pd^{2+} 3d_{3/2}$, respectively. The peaks demonstrate that both the $PdCl_2$ and the Pd nanoparticles coexist on the surface of $PdCl_2$@f-FWCNTs. The area of the $Pd^{2+} 3d_{5/2}$ peak is significantly larger than that of $Pd^0 3d_{5/2}$, which indicates that $PdCl_2$ is the primary compound in the palladium-decorating reaction. After reduction, the Pd particle presents a metallic state, as indicated by the peaks at 335.2 eV for $Pd^0 3d_{5/2}$ and at 340.7 eV for $Pd^0 3d_{3/2}$. The slight shift of the $Pd^0$3d peak in the $PdCl_2$@f-FWCNT curve to a lower binding energy, as compared with that of the Pd@f-FWCNTs, suggests a Pd−Cl interaction.

The ultraviolet photoelectron spectrometer (UPS) was used for measuring variations in work functions of CNTs after different treatments, as shown in Figure 4. The work function of the FWCNTs was 4.84 eV. It increased by 0.26 eV when Pd nanoparticles were successfully decorated onto the FWCNT surface to form Pd@f-FWCNTs with a work function of 5.10 eV. During the formation of Pd nanoparticles on the f-FWCNT surface, Pd^{2+} played the role of electron acceptor and received electrons from semiconducting SWCNTs mixed with the FWCNTs. The electrons in the SWCNTs were transferred to Pd^{2+}, which resulted in a decrease of the Fermi level of the f-FWCNTs because of the p-type doping effect.[33]

A useful index for evaluating the interface properties between metal particles containing Pd nanoparticles, metallic CNTs and semiconducting SWCNTs is the Schottky barrier height (SBH). There are two types of SBH, n-type and p-type SBH (p-SBH), and the Pd-CNT contact is considered a p-SBH. The p-SBH is defined as the difference between the work function of Pd and the top of the valence band of the semiconducting CNTs. The p-SBH affects the contact resistance between the metallic materials and the semiconducting

CNTs.[34] Therefore, the increase in the work function makes the p-SBH decrease and the Fermi level shift downward, which decreases the contact resistance.

Figure 5 presents a plot of the sheet resistance *versus* optical transmittance at wavelength of 550 nm for CNT-TCFs with varied thicknesses. The sheet resistance decreases with decreasing transmittance for all the materials studied in this work. Because of the Pd decoration on the f-FWCNT surface, the sheet resistance decreased from 6998 ohm/sq (estimated by the extrapolation method) for the pristine FWCNTs to 274 ohm/sq for the Pd@f-FWCNTs, with a corresponding transmittance of 81.65% at 550 nm. At a high transmittance, such as 98%, the decrease in the sheet resistance is more significant. A reduction of more than 2 orders of magnitude in the sheet resistance was detected. The entangled nature of the f-FWCNTs associated with interconnections created by the decorated Pd nanoparticles generates additional electrical paths, which lower the sheet resistance. Also, Pd decoration can enhance the p-type doping effect and decrease the p-SBH, which controls the contact resistance between the metal and semiconducting CNTs; consequently, the electrical conductivity of the CNT-TCFs increases.

CONCLUSIONS

This work demonstrates the processing of CNT-TCFs using Pd@f-FWCNTs as additives. During the Pd-decoration process, the f-FWCNTs were initially adhered by the Pd and $PdCl_2$ particles, and the latter were the primary adsorbate. After reduction in H_2, all the decorated particles on the surface of the f-FWCNTs were transferred to spherical Pd nanoparticles with average diameters of 5 nm. The decorated materials not only provide additional channels for electron transfer, but also decrease the contact resistance because of the p-type doping effect and the decrease in the SBH; as a result, increased the electrical conductivity of the CNT-TCFs. CNT-TCFs with extremely low sheet resistances of 274 ohm/sq and a high transmittance of 81.65% at a wavelength of 550 nm were achieved.

METHODS

Processing for Purified FWCNTs (p-FWCNTs). The as-purchased pristine FWCNTs (XinNano Materials, XNM-HP-12050, 4 nm average diameter, 86% purity) were oxidized in air at 600 °C for 1 h to remove the amorphous carbon, followed by treatment with hydrochloric acid (8 M) under stirring for 1 h to remove particles containing catalysts of metal oxide and metal particles. The product was then subjected to vacuum filtration through a filter (Millipore, 1 μm pore size, PTFE) and rinsed with copious amounts of pure water (10 MΩ) until a pH of 7 was reached (ECHO Chemical, litmus paper).[35,36]

Processing of Functionalized FWCNTs (f-FWCNTs). The wet p-FWCNTs were added to a mixture of concentrated sulfuric and nitric acid in a volume ratio of 3:1 under stirring for 2 h.[37] The product was collected by vacuum filtration and washed with copious amounts of pure water until the pH reach neutrality.

Palladate Decoration Reaction ($PdCl_2$@f-FWCNTs). To coat Pd particles on the surface of f-FWCNTs, the wet f-FWCNT powders were placed in an aqueous solution of 5 mM sodium tetrachloropalladate (Acros, Na_2PdCl_4) under stirring for 12 h. After filtration, the product was rinsed with pure water until neutrality was reached and then dried at 150 °C for 24 h. The dried powder was designated as $PdCl_2$@f-FWCNTs.

Palladate Reduction Process (Pd@f-FWCNTs). The reduction process was conducted under hydrogen gas (H_2, 99.99% in purity) in a tube furnace at 500 °C with at a flow rate of 2000 sccm for 30 min. The final product was designated as Pd@f-FWCNTs. Before and after the reduction processes, the furnace was purged with argon gas at a flow rate of 5000 sccm for 5 min.

Processing of CNT Ink. The starting materials of CNT ink were composed of 30 mg of Pd@f-FWCNTs, 120 mg of polyvinylpyrrolidone, and 200 mL of ethanol (ECHO Chemical, 99.99% in purity), which acted as a conductive material, a dispersant, and a solvent, respectively. The ink was prepared by mixing the starting materials, sonicating them (Branson 5210) for 1 h, and centrifuging at 10 000 rpm (Kubota 7780) for another 1 h. The black CNT ink was obtained from the upper layer of the centrifuged ink.

Processing of CNT-TCF. Poly(ethylene terephthalate) (PET, 91% in transmittance without any coating layer) film was adopted as the substrate and the wire-wound (Industry Tech, No. 9, the thickness of one layer is 22 μm) coating method was used to fabricate the CNT-TCFs.[38] The sheet resistance and transparency were controlled by coating the PET film for different numbers of layers. The coated layer on the PET substrate was dried in a box furnace at 150 °C for 15 min.

Characterization of CNT-TCF. The sheet resistance of CNT-TCF was measured using a conventional instrument (Mitsubishi Chemical MCP-T600). The optical transmittance was measured using a UV−vis spectrometer (Hitachi u-3410) in transmittance mode. The scanned wavelength range was from 350 to 750 nm in the visible region. The coated CNT-TCF samples were placed in the sample holder, and the noncoated PET was put in the reference holder as background. The transmittance performance of the CNT-TCFs studied in this work is independent from PET transmittance. The transmittance at 550 nm was used to estimate the optical transmittance of the CNT-TCFs.

Acknowledgment. This work was supported by the National Science Council under Grant No. NSC 98-2221-E-007-045-MY3. The authors would like to thank Prof. Yu-Tai Tao at Academia Sinica, Taiwan, for his support on the measurement of the UPS spectra of CNTs.

REFERENCES AND NOTES

1. Hanson, E. L.; Guo, J.; Koch, N.; Schwartz, J.; Bernasek, S. L. Advanced Surface Modification of Indium Tin Oxide for Improved Charge Injection in Organic Devices. *J. Am. Chem. Soc.* **2005**, *127*, 10058–10062.
2. Bardecker, J. A.; Ma, H.; Kim, T.; Huang, F.; Liu, M. S.; Cheng, Y.-J.; Ting, G.; Jen, A. K.-Y. Self-Assembled Electroactive Phosphonic Acids on ITO: Maximizing Hole-Injection in Polymer Light-Emitting Diodes. *Adv. Funct. Mater.* **2008**, *18*, 3964–3971.
3. Chae, J.; Appasamy, S.; Jain, K. Patterning of Indium Tin Oxide by Projection Photoablation and Lift-off Process for Fabrication of Flat-Panel Displays. *Appl. Phys. Lett.* **2007**, *90*, 261102.
4. Lee, S.; Noh, J. H.; Bae, S.-T.; Cho, I.-S.; Kim, J. Y.; Shin, H.; Lee, J.-K.; Jung, H. S.; Hong, K. S. Indium-Tin-Oxide-Based Transparent Conducting Layers for Highly Efficient Photovoltaic Devices. *J. Phys. Chem. C* **2009**, *113*, 7443–7447.
5. Andersson, A.; Johansson, N.; Bröms, P.; Yu, N.; Lupo, D.; Salaneck, W. R. Fluorine Tin Oxide as an Alternative to Indium Tin Oxide in Polymer LEDs. *Adv. Mater.* **1998**, *10*, 859–863.

6. Gamard, A.; Babot, O.; Jousseaume, B.; Rascle, M.-C.; Toupance, T.; Campet, G. Conductive F-Doped Tin Dioxide Sol-Gel Materials from Fluorinated β-Diketonate Tin(IV) Complexes. Characterization and Thermolytic Behavior. *Chem. Mater.* **2000**, *12*, 3419–3426.
7. Murdoch, G. B.; Hinds, S.; Sargent, E. H.; Tsang, S. W.; Mordoukhovski, L.; Lu, Z. H. Aluminum Doped Zinc Oxide for Organic Photovoltaics. *Appl. Phys. Lett.* **2009**, *94*, 213301.
8. Minami, T. Transparent Conducting Oxide Semiconductors for Transparent Electrodes. *Semicond. Sci. Technol.* **2005**, *20*, S35–S44.
9. Cairns, D. R.; Witte, R. P., II; Sparacin, D. K.; Sachsman, S. M.; Paine, D. C.; Crawford, G. P.; Newton, R. R. Strain-Dependent Electrical Resistance of Tin-Doped Indium Oxide on Polymer Substrates. *Appl. Phys. Lett.* **2000**, *76*, 1425–1427.
10. Zhang, F.; Johansson, M.; Andersson, M. R.; Hummelen, J. C.; Inganäs, O. Polymer Photovaltaic Cells with Conducting Polymer Anodes. *Adv. Mater.* **2002**, *14*, 662–665.
11. Kim, W. H.; Mäkinen, A. J.; Nikolov, N.; Shashidhar, R.; Kim, H.; Kafafi, Z. H. Molecular Organic Light-Emitting Diodes Using Highly Conducting Polymers as Anodes. *Appl. Phys. Lett.* **2002**, *80*, 3844–3846.
12. Kirchmeyer, S.; Reuter, K. Scientific Importance, Properties and Growing Applications of Poly(3,4-Ethylenedioxythiophene). *J. Mater. Chem.* **2005**, *15*, 2077–2088.
13. Vitoratos, E.; Sakkopoulos, S.; Dalas, E.; Paliatsas, N.; Karageorgopoulos, D.; Petraki, F.; Kennou, S.; Choulis, S. A. Thermal Degradation Mechanisms of PEDOT:PSS. *Org. Electron.* **2009**, *10*, 61–66.
14. Wu, Z.; Chen, Z.; Du, X.; Logan, J. M.; Sippel, J.; Nikolou, M. Transparent, Conductive Carbon Nanotube Films. *Science* **2004**, *305*, 1273–1276.
15. Paul, S.; Kim, D. W. Preparation and Characterization of Highly Conductive Transparent Films with Single-Walled Carbon Nanotubes for Flexible Display Applications. *Carbon* **2009**, *47*, 2436–2441.
16. Fanchini, G.; Unalan, H. E.; Chhowalla, M. Modification of Transparent and Conducting Single Wall Carbon Nanotube Thin Films *via* Bromine Functionalization. *Appl. Phys. Lett.* **2007**, *90*, 092114.
17. Parekh, B. B.; Fanchini, G.; Eda, G.; Chhowalla, M. Improved Conductivity of Transparent Single-Wall Carbon Nanotube Thin Films *via* Stable Postposition Functionalization. *Appl. Phys. Lett.* **2007**, *90*, 121913.
18. De, S.; Lyons, P. E.; Sorel, S.; Doherty, E. M.; King, P. J.; Blau, W. J. Transparent, Flexible, and Highly Conductive Thin Films Based on Polymer-Nanotube Composites. *ACS Nano* **2009**, *3*, 714–720.
19. Song, Y. I.; Yang, C. M.; Kim, D. Y.; Kanoh, H.; Kaneko, K. Flexible Transparent Conducting Single-Wall Carbon Nanotube Film with Network Bridging Method. *J. Colloid Interface Sci.* **2008**, *318*, 365–371.
20. Lee, S.; Kahng, S.-J.; Kuk, Y. Nano-Level Wettings of Platinum and Palladium on Single-Walled Carbon Nanotubes. *Chem. Phys. Lett.* **2010**, *500*, 82–85.
21. Yang, S. B.; Kong, B.-S.; Jung, D.-H.; Baek, Y.-K.; Han, C.-S.; Oh, S.-K.; Jung, H.-T. Recent Advances in Hybrids of Carbon Nanotube Network Films and Nanomaterials for Their Potential Applications as Transparent Conducting Films. *Nanoscale* **2011**, *3*, 1361–1373.
22. Guo, D.—J.; Li, H.-L. Electrochemical Synthesis of Pd Nanoparticles on Functional MWNT Surfaces. *Electrochem. Commun.* **2004**, *6*, 999–1003.
23. Oh, S.-D.; So, B.-K.; Choi, S.-H.; Gopalan, A.; Lee, K.-P.; Yoon, K. R.; Choi, I. S. Dispersing of Ag, Pd, and Pt—Ru Alloy Nanoparticles on Single-Walled Carbon Nanotubes by γ-Irradiation. *Mater. Lett.* **2005**, *59*, 1121–1124.
24. Park, H.; Kim, J.-S.; Choi, B. G.; Jo, S. M.; Kim, D. Y.; Hong, W. H.; Jang, S.-Y. Sonochemical Hybridization of Carbon Nanotubes with Gold Nanoparticles for the Production of Flexible Transparent Conducting Films. *Carbon* **2010**, *48*, 1325–1330.
25. Yang, S. B.; Kong, B.-S.; Geng, J.; Jung, H.-T. Enhanced Electrical Conductivities of Transparent Double-Walled Carbon Nanotube Network Films by Post-treatment. *J. Phys. Chem. C* **2009**, *113*, 13658–13663.
26. Liu, Y.-T.; Feng, Q.-P.; Xie, X.-M.; Ye, X.-Y. The Production of Flexible and Transparent Conductive Films of Carbon Nanotube/Graphene Networks Coordinated by Divalent Metal (Cu, Ca or Mg) Ions. *Carbon* **2011**, *49*, 3371–3391.
27. Kim, K. K.; Bae, J. J.; Park, H. K.; Kim, S. M.; Geng, H. Z.; Park, K. A. Fermi Level Engineering of Single-Walled Carbon Nanotubes by $AuCl_3$ Doping. *J. Am. Chem. Soc.* **2008**, *130*, 12757–12761.
28. Skákalová, V.; Kaiser, A. B.; Dettlaff-Weglikowska, U.; Hrnčarikov, K.; Roth, S. Effect of Chemical Treatment on Electrical Conductivity, Infrared Absorption, and Raman Spectra of Single-Walled Carbon Nanotubes. *J. Phys. Chem. B* **2005**, *109*, 7174–7181.
29. Rao, A. M.; Eklund, P. C.; Bandow, S.; Thess, A.; Smalley, R. E. Evidence for Charge Transfer in Doped Carbon Nanotube Bundles from Raman Scattering. *Nature* **1997**, *388*, 257–259.
30. Toebes, M. L.; van Dillen, J. A.; de Jong, K. P. Synthesis of Supported Palladium Catalysts. *J. Mol. Catal. A-Chem.* **2001**, *173*, 75–98.
31. Simonov, P. A.; Romanenko, A. V.; Prosvirin, I. P.; Moroz, E. M.; Boronin, A. I.; Chuvilin, A. L.; Likholobov, V. A. On the Nature of the Interaction of H_2PdCl_4 with the Surface of Graphite-like Carbon Materials. *Carbon* **1997**, *35*, 73–82.
32. Hasik, M.; Bernasik, A.; Drelinkiewicz, A.; Kowalski, K.; Wenda, E.; Camra, J. XPS Studies of Nitrogen-Containing Conjugated Polymers-Palladium Systems. *Surf. Sci.* **2002**, *507—510*, 916–921.
33. Kong, B.-S.; Jung, D.-H.; Oh, S.-K.; Han, C.-S.; Jung, H.-T. Single-Walled Carbon Nanotube Gold Nanohybrids: Application in Highly Effective Transparent and Conductive Films. *J. Phys. Chem. C* **2007**, *111*, 8377–8382.
34. He, Y.; Zhang, J.; Hou, S.; Wang, Y.; Yu, Z. Schottky Barrier Formation at Metal Electrodes and Semiconducting Carbon Nanotubes. *Appl. Phys. Lett.* **2009**, *94*, 093107.
35. Qian, C.; Qi, H.; Liu, J. Effect of Tungsten on the Purification of Few-Walled Carbon Nanotubes Synthesized by Thermal Chemical Vapor Deposition Methods. *J. Phys. Chem. C* **2007**, *111*, 131–133.
36. Yuan, D. Property Control of Single-Walled Carbon Nanotubes and Their Devices. Ph.D. Thesis, Duke University, Durham, NC, 2008, Chapter 5, 103—133.
37. Avilés, F.; Cauich-Rodríguez, J. V.; Moo-Tah, L.; May-Pat, A.; Vargas-Coronado, R. Evaluation of Mild Acid Oxidation Treatments for MWCNT Functionalization. *Carbon* **2009**, *47*, 2970–2975.
38. Dan, B.; Irvin, G. C.; Pasquali, M. Continuous and Scalable Fabrication of Transparent Conducting Carbon Nanotube Films. *ACS Nano* **2009**, *3*, 835–843.